Available online at www.sciencedirect.com
ScienceDirect
C. R. Chimie 11 (2008) 95–100
COMPTES RENDUS CHIMIE
http://france.elsevier.com/direct/CRAS2C/

Full paper / Mémoire

Preparation of nitrogen-doped titania with visible-light activity and its application

Hao-Li Qin [a,b], Guo-Bang Gu [a], Song Liu [a,*]

[a] College of Chemistry, South China University of Technology, Guangzhou 510640, PR China
[b] School of Science, Guizhou Normal University, Guiyang 550001, PR China

Received 8 December 2006; accepted after revision 6 June 2007
Available online 23 July 2007

Abstract

In order to utilize visible light in a photocatalytic reaction, yellow nitrogen-doped titania was prepared by sol–gel method in mild condition, with the elemental nitrogen source from ammonium carbonate. The catalysts were characterized by XRD, BET, and UV–vis diffuse reflectance spectrophotometry. The analytical results demonstrated that all catalysts were anatase, and the crystallite size of nitrogen-doped titania increased with increasing N/Ti proportioning, and the doping of nitrogen could enlarge the specific surface, extending the absorption shoulder into the visible-light region. Photocatalytic activity of the nitrogen-doped titania catalysts was evaluated based on the photodegradation of methyl orange and 2-mercaptobenzothiazole in aqueous solution under visible light. The effect of preparation conditions such as N/Ti proportion and calcination temperature on the visible-light activity was also discussed. The experiments demonstrated that the nitrogen-doped titania with N/Ti proportioning of 20 mol% calcined at 400 °C exhibited the highest visible-light activity. It was concluded that the enhancement of methyl orange and 2-mercaptobenzothiazole photodegradation using the nitrogen-doped titania catalysts is mainly involved in the enhancement of the separation of electron–hole pairs owing to the presence of Ti^{3+}, the improvement of the organic substrate adsorption in catalysts suspension and optical response in visible-light region. ***To cite this article: H.-L. Qin et al., C. R. Chimie 11 (2008).***

Keywords: Titania; Nitrogen-doped; Visible light

1. Introduction

Titania is well known as a cheap, stable, nontoxic, and efficient photocatalyst without secondary pollution. However, because of the relatively high intrinsic band gap of anatase TiO_2 (3.2 eV), only 4% of the incoming solar energy on the Earth's surface can be utilized. On the other hand, the hole and electron excited by the UV light can recombine easily, which will reduce the efficiency of photons. How to reduce the band gap to produce the visible-light photocatalysis and suppress the recombination of hole-electron pairs has been one of the most challenging topics [1]. Therefore, considerable efforts have been made to extend the photoactivity of titania-based systems into the visible-light region, using dopants. Regarding nitrogen-doped titania, Sato [2] reported for the first time that a titania-based

* Corresponding author.
E-mail address: chsliu@scut.edu.cn (S. Liu).

1631-0748/$ - see front matter © 2007 Académie des sciences. Published by Elsevier Masson SAS. All rights reserved.
doi:10.1016/j.crci.2007.06.004

material from the mixtures of a commercial titanium hydroxide and ammonium calcined at about 400 °C showed higher photocatalytic activity in the visible-light region. Recently, many researchers paid much attention to nitrogen-doped titanias which have been produced through different techniques, such as hydrolytic process [4–7], mechanochemical technique [8–10], reactive DC magnetron sputtering [11,12], high-temperature treatment of titania under NH_3 flow [3,13,14], sol–gel method [15], solvothermal process [16] and calcination of a complex of Ti^{4+} with a nitrogen-containing ligand [17]. Generally, the elemental nitrogen was mostly derived from ammonium [3,13,14,18] and urea [19–21].

In this study, we incorporated nitrogen into titania by sol–gel method in mild condition, using tetrabutyl titanate as the titanium source and ammonium carbonate as the nitrogen source. The titania catalysts were characterized by XRD, BET, and UV–vis diffuse reflectance spectrophotometry. The nitrogen-doped titania photocatalysts were found to be more active for methyl orange (MO) and 2-mercaptobenzothiazole (MBT) degradation under visible-light irradiation compared to undoped ones. The effect of N/Ti proportioning and calcination temperature on the visible-light activity was also discussed.

2. Experimental methods

2.1. Synthesis

In a typical preparation procedure, 17 ml of tetra-*n*-butyl titanium ($Ti(O–Bu)_4$) was dissolved in 40 ml of absolute ethanol and then this $Ti(O–Bu)_4$ solution was added drop-wise under vigorous stirring into 55 ml of the mixture solution containing 40 ml of absolute ethanol, 10 ml glacial acetic acid, and 5 ml of double-distilled water. The resulting transparent colloid was stirred for 0.5 h and aged for 2 days till the formation of xerogel, then grounded into powders. The powders were calcined at 400 °C for 3 h, then grounded in agate mortar and screened by shaker to obtain finally fine titania powders (signed as t400-0#). Other undoped titania calcined at 450 °C and 500 °C were signed as t450-0# and t500-0#, respectively.

A series of nitrogen-doped titania catalysts calcined at 400 °C were generated with the following procedure: different volumes of 1 mol/l ammonium carbonate (corresponding to different N/Ti proportioning of 4, 8, 12, 20, 24, 28, and 32 mol% signed as t400-1#, t400-2#, t400-3#, t400-4#, t400-5#, t400-6#, and t400-7#, respectively) were added into the resulting transparent colloid under vigorous stirring and stirred for 1 h, then aged for 2 days till the formation of xerogel. The following procedure was carried out according to the undoped titania. Other nitrogen-doped titania catalysts calcined at 450 and 500 °C were signed as above.

2.2. Characterization

X-ray diffraction (XRD) patterns were recorded using a Shimadzu XD-3A diffractometer with Cu Kα radiation. An accelerating voltage of 30 kV and emission current of 30 mA were applied. The absorption edges of catalysts were determined from the onset of the diffuse reflectance spectrum using a UV–vis spectrophotometer equipped with an integrated sphere (Hitachi, UV-3010). The specific surface area of some samples was measured by the Brunauer–Emmett–Teller (BET) method, in which the N_2 adsorption at 77 K using ASAP 2010 was applied. The pore size distribution of the catalysts was determined by the Barrett–Joyner–Halenda (BJH) method. The photooxidation products of sulfate ion, nitrate ion, and ammonium ion were determined by ion chromatography with a conductivity detector (DIONEX, ICS-1000 for cationic ion, and ICS-90 for anionic ion), in which a AS12A anionic column and mobile phase containing 9 mM Na_2CO_3 were used for determination of sulfate and nitrate ions, while a IonPac CS12A cationic column and a mobile phase containing 11 mM H_2SO_4 were used for the determination of the ammonium ion.

2.3. Photoreactor system

The photocatalyst's activity was evaluated using the photocatalytic degradation of MO and MBT under a 200-W tungsten halide lamp (THL) as the visible-light source. The THL was out of the reactor. The reactor was surrounded by a borosilicate glass jacket with 2 mol/l $NaNO_2$ aqueous solution [22] cycling inside. An $NaNO_2$ aqueous solution was used to avoid the UV light. For each experiment, 0.2 g photocatalyst was added to 200 ml of 5 mg/l MO or MBT solution stirred with a magnetic stirrer, and air was bubbled through the reaction media during the experiments. Before irradiation, suspensions were stirred for 3 h in the dark to ensure equilibrium of the solution with the photocatalyst. The concentration of aqueous MO and MBT was determined with a Hitachi UV-3010 spectrometer by measuring the absorbance at 464 and 316.5 nm, respectively. For comparison, a photocatalytic reaction was also carried out using commercial titania (Degussa P-25).

The chemical structure of MO and MBT was listed as follows:

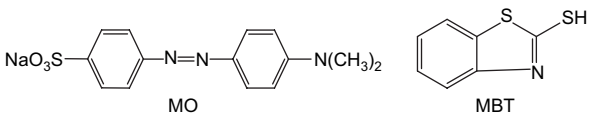

3. Results and discussion

3.1. Crystal phase composition

Fig. 1 shows the XRD patterns of the samples. It can be seen from Fig. 1 that all samples are in anatase phase. Neither specific peaks of Ti–N nor of N–O were detected. Average grain sizes calculated from the broadening of the (101) peak of anatase phase were 7.2, 13.4, 14.6 and 28.8 nm for t400-0#, t400-3#, t400-4# and t400-7#, respectively. The doping of elemental nitrogen resulted in the enlargement of the crystallite size, and the crystallite size increased with increasing N/Ti proportioning.

3.2. Surface area and pore size of photocatalysts

To investigate the effects of doping on the pore structure and adsorption property of samples, a set of nitrogen adsorption–desorption tests were carried out and their isotherms are presented in Fig. 2. It could be seen from Fig. 2 that the isotherms of undoped titania and nitrogen-doped titania (t400-4# and t400-7#) all showed a typical shape of Type IV (BDDT classification) [23]. Undoped titania had a gentle hysteresis loop of Type H2 at relative pressure from 0.4 to 0.8, while nitrogen-doped titania t400-4# showed precipitous and narrow hysteresis loops at relative pressure from 0.4 to 0.8. The BET surface areas of titania catalysts calcined at 400 °C were 132.76, 98.60, 61.18 m^2/g for t400-4#, t400-7# and t400-0#, respectively. The data of larger BET specific surface area and larger crystal size indicated that nitrogen-doped titania had a more porous structure than that of undoped ones. The above results also indicated that all titania prepared by sol–gel method had a mesoporous structure.

The pore size distribution determined by the BJH method shown in Fig. 3 indicated that undoped titania had mainly a ordered mesoporous structure and its pore size was in the main range of 2.0–7.0 nm with a maximum portion at about 4 nm. The pore size

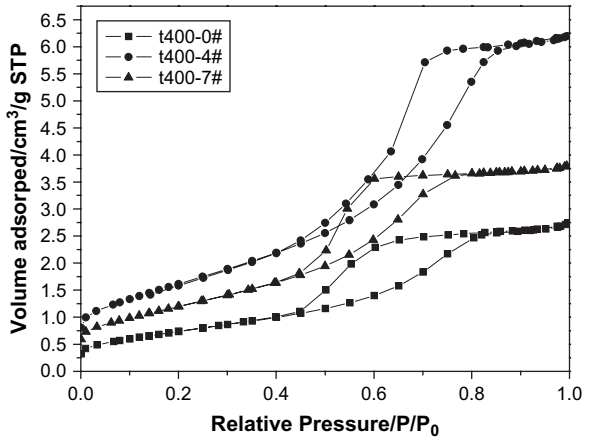

Fig. 2. Nitrogen adsorption–desorption isotherms of nitrogen-doped titania.

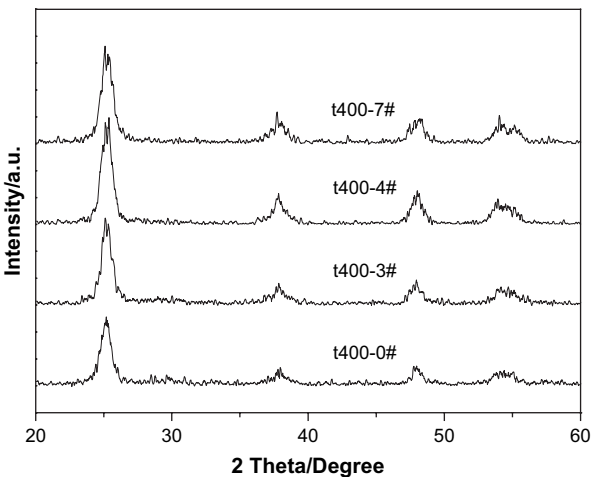

Fig. 1. XRD patterns of different titania catalysts calcined at 400 °C.

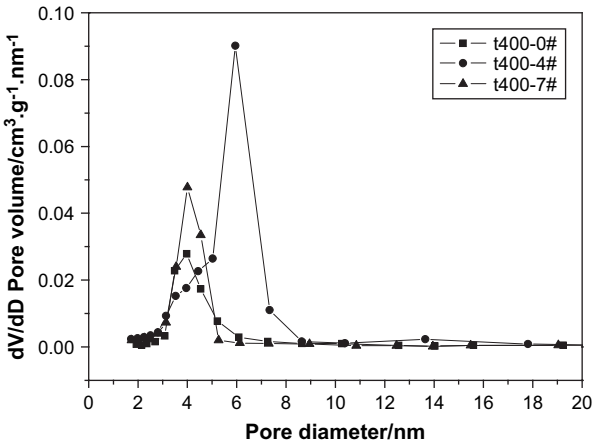

Fig. 3. Pore size distribution of catalyst calculated by the BJH method.

distribution of t400-4# showed larger range of 2.0–9.0 nm with a maximum portion at about 6 nm. The results showed that the pore size of all samples was uniform in the range of 0–10 nm and that nitrogen-doped titania had larger pore size than undoped ones. These mesoporous structure was attributed to the pores formed between catalyst particles [24,25]. The decomposition of ammonium carbonate and release of ammonia and carbon dioxide during the process of calcination resulted in a more abundant formation of mesoporous structure of nitrogen-doped titania than of the undoped one.

3.3. Diffuse reflectance spectrum of photocatalysts

The diffuse reflectance spectra of catalysts prepared under different conditions are shown in Fig. 4. The same absorption edges were observed for undoped titania and the nitrogen-doped ones, but a noticeable shift of the absorption shoulder extending to the visible-light region was observed for the nitrogen-doped titania catalyst. Asahi et al. [3] and other investigators [8,10,16] reported that the optical absorption edge shifted to visible-light region and proved that mixing of the N_{2P} and O_{2P} states narrowed the band gap. However, our results were different from theirs. The UV–vis spectra proved that an isolated narrow N_{2P} band was above the valence band [13], so there was no shift in the optical absorption edge between the nitrogen-doped and undoped titania. In the visible-light region ($\lambda > 400$ nm), the optical absorption intensity is different, depending on the calcination temperature. As shown in Fig. 4, the visible-light absorbance decreased as the calcination temperature increased. As reported in the literature [13], the nitrogen incorporated in the lattice of TiO_2 can cause photocatalyst to respond to visible light. The nitrogen is burnt out at elevated temperature, reducing the absorbance of visible light. In addition, the color of undoped titania was white, whereas that of the nitrogen-doped titania was yellow. It implied that the optical absorption intensity had something to do with the shade of color: the darker the color, the higher the optical absorption intensity.

3.4. Evaluation of photocatalytic activity

Fig. 5(a)–(c) shows photodegradation of MO in the presence of titania calcined at 400, 450, and 500 °C under irradiation of visible light, and Fig. 5(d) shows photodegradation of MBT with titania calcined at 400 °C. The MO and MBT degradation rate of blank test without any photocatalysts was zero. It was obvious that the visible-light activities of nitrogen-doped titania were better than that of undoped one, and the titania catalysts calcined at 400 °C showed better photocatalytic activity. The higher the calcination temperature was, the worse the visible-light activity was. The t400-4# catalyst demonstrated the highest visible-light activity. From Fig. 5(a) and (d), it was clear that the visible-light activity of nitrogen-doped titania was much higher than that of commercial Degussa P-25.

To evaluate the conversion of organic sulfur and nitrogen in the MBT photocatalytic degradation under irradiation of visible light, a test was carried out in the suspension containing catalysts (t400-4#) and MBT (50 mg/l) for 300 min. The experimental results are shown in Fig. 6 that the concentrations of sulfate-S, ammonium-N, and nitrate-N increased from 0 to 7.19, 1.37, and 0.72 mg/l, respectively. The conversion of

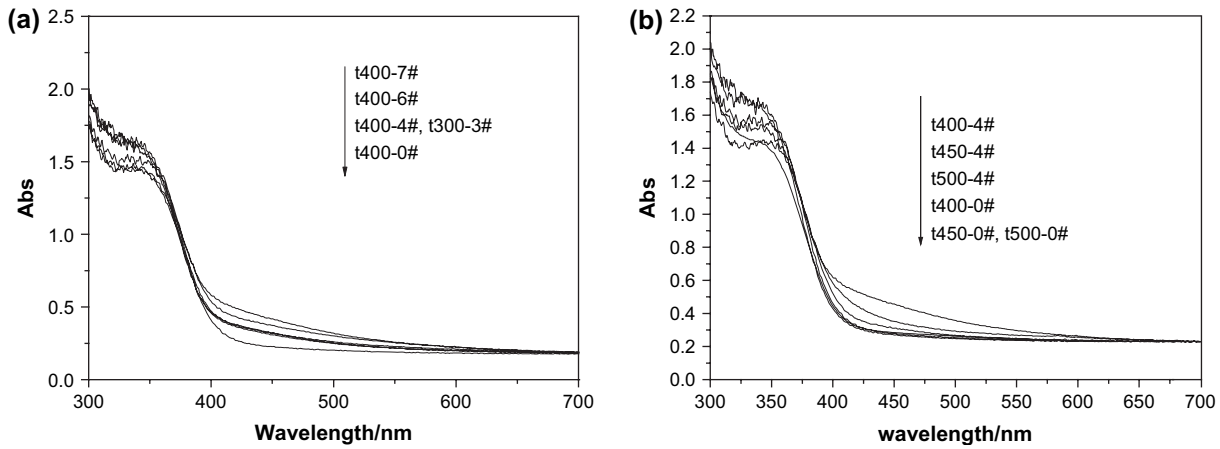

Fig. 4. UV–vis absorption spectra of titania catalysts calcined at (a) 400 °C and (b) different temperatures.

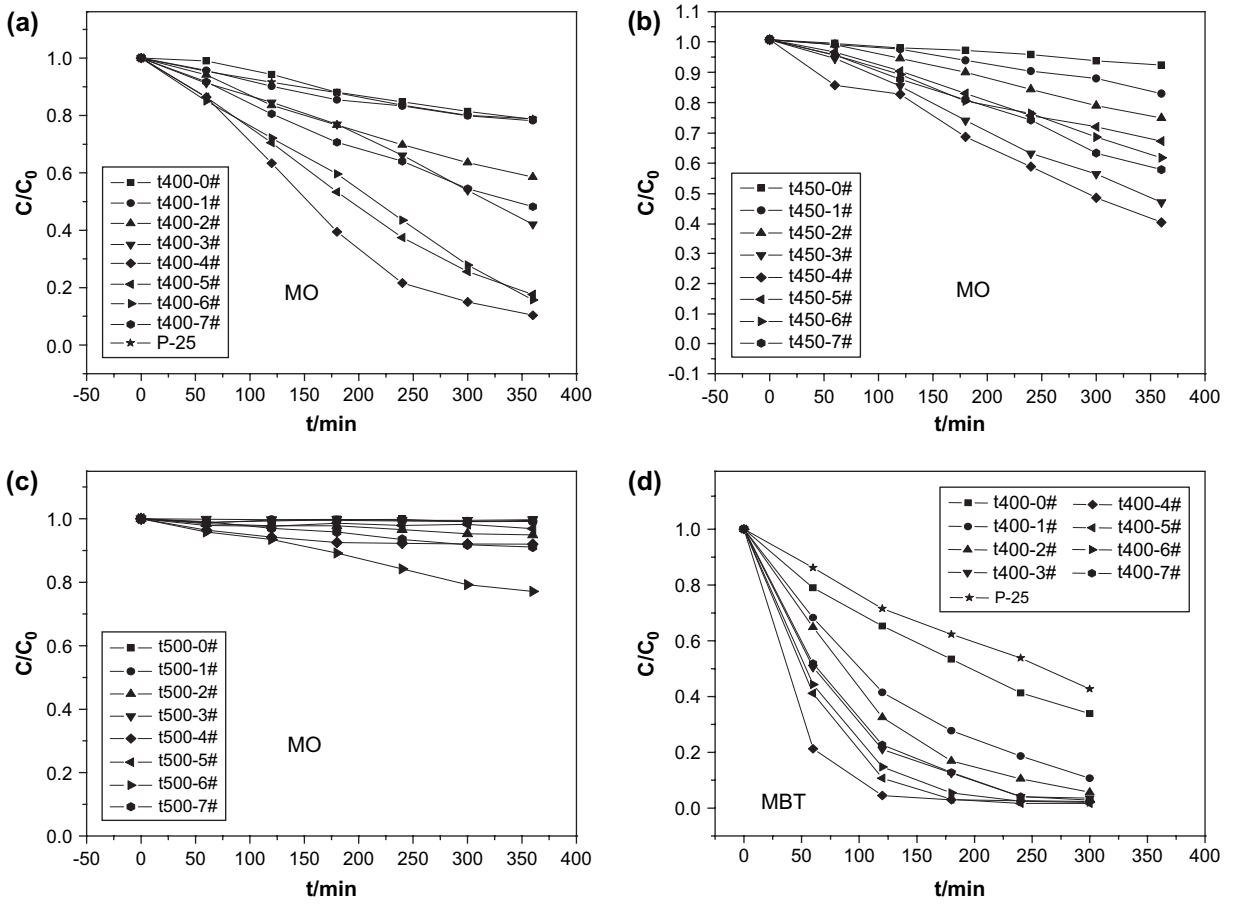

Fig. 5. Photocatalytic degradation of MO with TiO_2 calcined at (a) 400 °C, (b) 450 °C, (c) 500 °C, and (d) photocatalytic degradation of MBT with TiO_2 calcined at 400 °C.

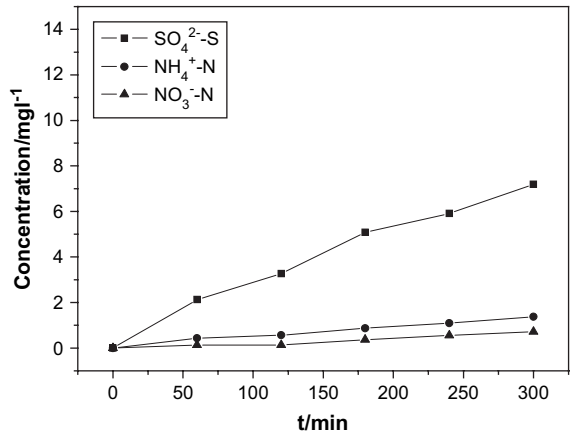

Fig. 6. Formation of sulfate, ammonium and nitrate ions during MBT photocatalytic degradation with catalysts (t400-4#).

organic sulfur and organic nitrogen was achieved by 37.6 and 17.2%, respectively.

It was found in this study that the crystal composition of the photocatalysts was anatase. Alternatively, the modification of the surface state of the catalysts might be another critical reason for promoting the effective separation of electron–hole pairs and photoactivity. In the nitrogen-doped titania catalysts, the oxygen sites were partially replaced with nitrogen atoms, while TiO_2 was simultaneously reduced [23]. These changes caused an increase in oxygen vacancy and amount of Ti^{3+}. The electrons and holes were generated in the initial stage of visible-light illumination, and the defects on the titania surface or in the bulk could suppress the recombination of electron–hole pairs and hence extend their lifetime [24]. As the concentration of dopant increased, the more TiO_2 was reduced and the amount of oxygen vacancies increased. When the concentration

of dopant was excessively high, the space charge region became very narrow and the penetration depth of light into titania greatly exceeded the space charge layer; therefore, the recombination of the photogenerated electron–hole pairs became easier [25]. Here, excessive oxygen vacancy and Ti^{3+} acted as a recombination center for holes and electrons [13], which explained why an optimal content of Ti^{3+} existed on the nitrogen-doped titania. Therefore, the presence and optimal content of Ti^{3+} might be the critical factors leading to the improvement of the photoactivity.

On the other hand, larger specific surface area and larger pore size induced by doping would enhance the adsorption capacity of nitrogen-doped titania for organic substrates, which is of benefit to the photocatalytic reaction. In addition, optical absorbance intensity in visible-light region of catalysts was also an important factor to influence the visible-light activity of catalysts. Considering the correlation of the absorbance in visible-light region to visible-light activity of nitrogen-doped titania as shown in Figs. 4 and 5, it can be seen that the stronger the optical absorbance intensity is, the higher the photocatalytic activity is. Compared with undoped titania, nitrogen-doped titania has larger surface area, larger pore size and stronger optical absorbance intensity in visible-light region, which leads to a better visible-light activity.

4. Conclusions

Yellow nitrogen-doped titania catalysts, with the elemental nitrogen source from ammonium carbonate, were prepared using sol–gel method in mild conditions. The crystallite size of anatase nitrogen-doped titania was larger than the undoped one, and increased with increasing N/Ti proportioning. The nitrogen incorporated in the lattice of TiO_2 formed a narrow N_{2P} band above the valence band which exhibited higher visible-light absorption and was responsible for the visible-light activity. The amount of oxygen vacancy and Ti^{3+} on the surface of catalysts, specific surface area and optical adsorption intensity were all the factors that influence the photoactivities. The nitrogen-doped titania with N/Ti proportioning of 20 mol% calcined at 400 °C exhibited the highest visible-light activity.

Acknowledgements

This work was supported under Open Funds awarded by the Key Lab of Enhanced Heat Transfer and Energy Conservation, Ministry of Education, China.

References

[1] K. Vinodgopal, P.V. Kamat, Environ. Sci. Technol. 29 (1995) 841.
[2] S. Sato, Chem. Phys. Lett. 123 (1986) 126.
[3] R. Asahi, T. Morikawa, T. Ohwaki, K. Aoki, Y. Taga, Science 293 (2001) 269.
[4] Y. Sakatani, H. Koike, H. Koike, JP 2001072419, 2001-01–03.
[5] T. Ihara, M. Miyoshi, Y. Iriyama, O. Matsumoto, S. Sugihara, Appl. Catal. B: Environ. 42 (2003) 403.
[6] H. Noda, K. Oikawa, T. Ogata, K. Matsuki, H. Kamada, Nippon Kaaaku Zasshi 8 (1986) 1084.
[7] S. Salthivel, H. Kisch, ChemPhysChem 4 (2003) 487.
[8] S. Yin, H. Yamaki, M. Komatsu, Q.W. Zhang, J.S. Wang, Q. Tang, F. Saito, T. Sato, J. Mater. Chem. 13 (2003) 2996.
[9] S. Yin, H. Yamaki, Q.W. Zhang, M. Komatsu, J.S. Wang, Q. Tang, F. Saito, T. Sato, Solid State Ionics 172 (2004) 205.
[10] J.S. Wang, S. Yin, M. Komatsu, Q.W. Zhang, F. Saito, T. Sato, Appl. Catal. B: Environ. 52 (2004) 11.
[11] T. Lindgren, J.M. Mwabora, E. Avendano, J. Jonsson, A. Hoel, C.G. Granqvist, S.E. Lindquist, J. Phys. Chem. B 107 (2003) 5709.
[12] S.Z. Chen, P.Y. Zhang, W.P. Zhu, D.M. Zhuang, Chin. J. Catal. 25 (2004) 515.
[13] H. Irie, Y. Watanabe, K. Hashimoto, J. Phys. Chem. B 107 (2003) 5483.
[14] O. Diwald, T.L. Thompson, T. Zubkov, E.G. Goralski, S.D. Walck, J.T. Tates, J. Phys. Chem. B 108 (2004) 6004.
[15] C. Burda, Y. Lou, X. Chen, A.C.S. Samia, J. Stout, J.L. Gole, Nano Lett. 3 (2003) 1049.
[16] Y. Aita, M. Komatsu, S. Yin, T. Sato, J. Solid State Chem. 177 (2004) 3235.
[17] T. Sano, N. Negishi, K. Koike, K. Takeuchi, S. Matsuzawa, J. Mater. Chem. 14 (2004) 380.
[18] H.M. Yates, M.G. Nolan, D.W. Sheel, M.E. Pemble, J. Photochem. Photobiol. A: Chem. 179 (2006) 213.
[19] J. Yuan, M.X. Chen, J.W. Shi, W.F. Shangguang, Int. J. Hydrogen Energy 31 (2006) 1326.
[20] Y. Yanmamoto, S. Moribe, T. Ikoma, K. Akiyama, Q. Zhang, F. Saito, S. Tero-Kubota, Mol. Phys. 104 (2006) 1733.
[21] S. Yin, H. Yamaki, M. Komatsu, Q.W. Zhang, J.S. Wang, Q. Tang, F. Saito, T. Sato, Solid State Sci. 7 (2005) 1479.
[22] L. Christian, H. Kunt, K. Horst, W. Macyk, W.F. Maier, Appl. Catal. B: Environ. 32 (2001) 215.
[23] C.H. Shin, G. Bugli, G.D. Mariadssou, J. Solid State Chem. 95 (1991) 145.
[24] A.L. Linsebiger, G. Lu, J.T. Yatas, Chem. Rev. 95 (1995) 735.
[25] F.B. Li, X.Z. Li, M.F. Hou, Appl. Catal. B: Environ. 48 (2004) 185.